Natural Resources for Human Health
eISSN: 2583-1194

Original Research
Received 10 May 2026
Revised 15 June 2026
Accepted 28 June 2026

Natural Resources for Human Health 2026, Vol. 6 (11s): 866–881

KEYWORDS:
Maternal exposure, Sulforaphane, Risperidone, *St8sia2* and *St8sia4* genes, Gene expression, Rat brain development, Histological analysis, PAS staining

The Effect of Risperidone on the Expression of the *St8sia2* and *St8sia4* Genes and its effect on the Glycoproteins in the Brain Tissues of Embryos and Offspring of Albino Rats

[1]Shelan Qader Sadeq, [2]Zubaida Adnan Kudair

[1]Tikrit University / College of Education for Women / Department of Biology
[2]Tikrit University / College of Education for Pure Sciences / Department of Life Sciences
E-mail: shmscbio@tu.edu.iq, zubaida.biology@tu.edu.iq

ABSTRACT: The present study investigated the effects of maternal exposure to sulforaphane (SFN) and risperidone (RIS) during pregnancy and the early postnatal period on the expression of the sialyltransferase genes *St8sia2* and *St8sia4* and the histological characteristics of developing rat brain tissue at embryonic day 14 (E14), the day of birth (P0), and postnatal day 7 (P7).

RT-qPCR results showed differences in the expression levels of the ***St8sia2*** and ***St8sia4*** genes among the experimental groups across the developmental stages. For ***St8sia2***, no significant differences were observed between the Saline and SFN groups at any stage, whereas significant differences were detected between the RIS and SFN groups at **E14 (*P* = 0.0488)**, between the Saline and RIS groups at **P0 (*P* = 0.0360)**, and between the RIS and SFN groups at P0 (***P* = 0.0173**). At **P7**, significant differences were observed between the Saline and RIS groups (***P* = 0.0012**) and between the RIS and SFN groups (***P* = 0.0001**). For ***St8sia4***, no significant differences were observed among the experimental groups at **E14** or **P0**, whereas significant differences were detected at **P7** between the Saline and RIS groups (***P* = 0.0139**) and between the RIS and SFN groups (***P* = 0.0004**). Histological examination using PAS staining revealed positive staining in all experimental groups, particularly in the intercellular matrix, neuronal membranes, and vascular structures, consistent with the presence of glycoprotein-rich components in developing brain tissue. At E14, the Saline group showed an organized cellular architecture, the SFN group showed a more intense PAS reaction and the RIS group a moderate reaction. At P0 and P7, capillary basement membranes stained strongly across all groups; at P7, PAS reactivity was most intense in the SFN group, strong-to-moderate in the Saline group, and weakest in the RIS group.

Conclusion: Maternal exposure to RIS was associated with reduced *St8sia2* gene expression at P0 and P7 and reduced *St8sia4* expression at P7, compared with the Saline and/or SFN groups; however, developmental physiological factors may also influence this expression, and causality cannot be inferred. Sulforaphane did not significantly change the expression of either gene compared with the Saline (control) group. PAS staining showed glycoprotein-rich components in the developing brain of all groups, with differences in staining intensity that may reflect changes in glycoprotein content related to the glycocalyx.

Natural Resources for Human Health
eISSN: 2583-1194

INTRODUCTION

The brain is a highly complex organ comprising millions of neurons that control and regulate the body; communication between individual neurons and their interaction with glial cells are essential for proper brain function. Every cell in the human body is coated by a glycocalyx, a carbohydrate-rich layer of glycoproteins and glycolipids that mediates cell-cell and cell-matrix interactions. Tissues of every type, whether endothelial, immune, muscle, blood, or neuronal cells exhibit a glycocalyx, which encodes a vast array of information critical to both health and disease and can be directly targeted in therapeutic contexts (Möckl, 2020). Sugars located at the outer termini of glycan chains often dictate the functional specificity of glycans. In mammals, glycoproteins and glycolipids frequently terminate with sialic acids—essential sugars typically found at the distal ends of glycans—enabling them to act as bridging molecules between cells, and between cells and the extracellular matrix (Schnaar et al., 2014; Yoo et al., 2015). The glycocalyx is considered one of the most significant discoveries in histology and cell biology. The concept originated in the early 20th century when scientists observed a gelatinous coating covering cells; however, its chemical nature remained unclear until the mid-20th century (Richter and Sanderson, 2023; Foote et al., 2022). The covalent addition of sialic acid to the termini of glycoproteins is known as sialylation; this critical biological modification plays a role in embryonic and neuronal development. During this process, sialic acid is added to the terminal ends of glycan chains on the cell membrane by a family of enzymes called sialyltransferases specifically *St8sia2* and *St8sia4*. These enzymes polysialylate the glycans of a small subset of mammalian proteins; their most abundant substrate is the neural cell adhesion molecule (NCAM). They are responsible for adding polysialic acid (PSA/polysia) to various neuronal surface glycoproteins, thereby playing a central role in the formation of the neuronal glycocalyx. Polysialylation of NCAM modulates cell adhesion, neuronal migration, and synaptic plasticity during brain development (Zhu et al., 2024).

Risperidone is a widely prescribed atypical antipsychotic medication; however, maternal exposure to risperidone during pregnancy may alter fetal neurodevelopmental trajectories (Singh et al., 2016). Conversely, sulforaphane, a bioactive phytochemical derived from cruciferous vegetables, exhibits notable antioxidant and neuroprotective properties that may have a different effect on developmental outcomes (Bessetti and Litwa, 2025). Despite the well-established roles of *St8sia2* and *St8sia4* in early brain development, the comparative and longitudinal impacts of maternal exposure to risperidone and sulforaphane on these sialyltransferase genes and brain cell-surface glycocalyx layer remain insufficiently elucidated. Therefore, this study aimed to evaluate the effects of maternal administration of risperidone and sulforaphane during gestation and early postnatal periods on *St8sia2* and *St8sia4* gene expression, as well as histological characteristics of rat brain tissue at embryonic day 14 (E14), postnatal day 0 (P0), and postnatal day 7 (P7).

MATERIALS AND METHODS

Study Samples

This study utilized 18 healthy adult female albino laboratory rats *Rattus norvegicus*, obtained from the laboratory animal breeding unit at the College of Veterinary Medicine, Tikrit University. The rats ranged in age from 11 to 12 weeks and in weight from (225 ± 10) grams. They were housed under standard laboratory conditions, including a temperature of 22–25°C and a 12-hour light/12hour dark cycle, with continuous access to food and water.

Experimental Design

Mating was confirmed by the presence of vaginal plug, designated as Gestational Day 1 (GD1). Pregnant dams were randomly assigned into three experimental groups and housed in clean plastic cages. Treatments were administered daily via oral gavage from Gestational Day 7 (GD7) through Postnatal Day 7 (P7). Animal weights and general physical condition were monitored continuously for any clinical signs of adverse drug reactions.

Materials Administered to Rats

Pregnant rats were treated daily by oral gavage (1 ml/rat) from Gestational Day 7 to Postnatal Day 7 in three separate groups. The control group received standard physiological saline solution (NaCl) with a standard concentration of 0.9 %. The sulforaphane group received DL-sulforaphane 97%; (Cat. No. D818039; Macklin Biochemical Co., Ltd., Shanghai, China; Macklin Biochemical, 2025a) at a dose of (0.5 mg/rat/day). The Risperidone group received raw risperidone (Cat. No. R832185; Macklin Biochemical Co., Ltd., Shanghai, China; Macklin Biochemical, 2025b) at a dose of (0.5 mg /rat/ day). This dosage was selected based on previous developmental toxicity studies and corresponds to human therapeutic dose ranges (Singh et al., 2016; Singh and Singh, 2017; Okab et al., 2025).

Natural Resources for Human Health
eISSN: 2583-1194

Sample Collection Method

A total of 102 samples were collected across three distinct time points to investigate molecular developmental changes in the three experimental groups. Animals were anesthetized using a chloroform solution. Fetal brains were collected on embryonic day 14 (E14): Pregnant dams (two per group) were dissected under sterile conditions; the uterus was opened, and the fetuses were carefully extracted. Brains were then isolated using appropriate, precision dissection tools under conditions designed to preserve sample integrity. Neonatal rat brains were collected immediately after birth—postnatal day 0 (P0). Half of the pups from each group were separated from their mothers, anesthetized, and euthanized, while the remaining half were kept until one week after birth. Brains were then isolated from the neonates and preserved. Brains from young rats were collected one week after birth postnatal day 7 (P7) (comprising the second half of the pups, which had been reared and suckled by mothers that continued to receive the three experimental substances). These pups were separated from their mothers, anesthetized, and euthanized; their brains were then isolated using appropriate dissection tools under conditions ensuring sample preservation.

Sample Distribution According to Type of Analysis

Following extraction from the fetuses and newborns, the brains were divided into sections for the required tests, as follows: Brain tissue samples were preserved in Trizol solution and subsequently transferred to a deep freezer for storage at temperatures ranging from -20°C to -80°C; a total of 84 samples (derived from rat embryos and neonates) were collected for RNA extraction and molecular analysis specifically, the measurement of gene expression levels—using primers specific to the genes under investigation (*St8sia2* and *St8sia4*). Additionally, whole brain samples (18 in total) were preserved in 10% formalin for histological examination using the Periodic Acid-Schiff (PAS) stain to assess the presence and distribution of glycoproteins in brain tissue cells.

Molecular Analysis

Specific primers were designed to detect and quantify the expression of the genes under study—specifically the sialyltransferase genes *St8sia2* and *St8sia4*—using the NCBI Primer-BLAST tool; these primers were synthesized by Macrogen Inc. (Seoul, South Korea), as detailed in Table (1). Gene expression analysis was conducted on the three groups of rats to assess expression levels; this work was performed at the Central Laboratories Department at Tikrit University using a real-time PCR (RT-qPCR) system, with RNA extraction carried out using the TransZol Up Plus RNA Kit supplied by TRANS.

Table (1) Primer sequences used in the study, obtained using the Primer-BLAST tool available on the NCBI website.

Annealing °C	Size	Length	Sequence (5′-3′ direction)	Target Gene
Gene Expression Primers				
59	110	20	F- AGCACAATGAACGTGTCCCA	*St8sia2*
59	110	20	R- AGCAAGACTCCTGAGTTGCC	
59	110	20	F- ATAGCCAGGACTGAGGAGCA	*St8sia4*
59	110	20	R- GAACCAGCCTTCCGAGTGAT	
Housekeeping Gene				
59	143	20	F- GGAGAAACCTGCCAAGTATG	GAPDH
59	143	21	R- TGATGGTATTCGAGAGAAGGG	

RNA was converted into complementary DNA (cDNA) using the activity of the reverse transcriptase enzyme. Following the additions, the samples were transferred to a thermocycler, and the reaction was initiated according to the program outlined in Table (2).

Table (2) RT-qPCR reaction program

Step	Time(min-sec)	Temp. °C	Cycle
Enzyme activation	60 sec	95	1
Denaturation	15 sec	95	40-45
Extension	30 sec	60	-
Melt Curve	5 sec	60-90	1

Gene Expression

To measure the level of gene expression, the following equations were used (Livak and Schmittgen, 2001): Analysis of relative gene expression data using real-time quantitative PCR and the $2^{(-\Delta\Delta Ct)}$ method.

Histological Examinations

Upon completion of the dosing period for the rat groups under study, the animals were anesthetized with chloroform and dissected. The target organs—specifically the brains of the fetuses and newborns—were excised, and histological sections were prepared according to the methods of (Al-Hajj ,2010).

Statistical Analysis

Gene expression data for the *St8sia2* and *St8sia4* genes were analyzed using GraphPad Prism (Version 10) software. One-way ANOVA was employed to compare experimental groups at each time point individually, while two-way ANOVA was used to analyze differences between experimental groups across the three developmental stages. Tukey's multiple comparisons test was conducted to determine differences between groups. Results are presented as mean ± standard deviation (Mean ± SD), with a P-value < 0.05 considered statistically significant.

RESULTS

Using the RT-qPCR technique and the GAPDH gene as a reference across all 84 samples from the three experimental groups (RIS, SFN, and Saline), the melting curves exhibited sharp definition and narrow peaks—indicating the production of homogeneous and pure PCR products—as illustrated in Figure (1).

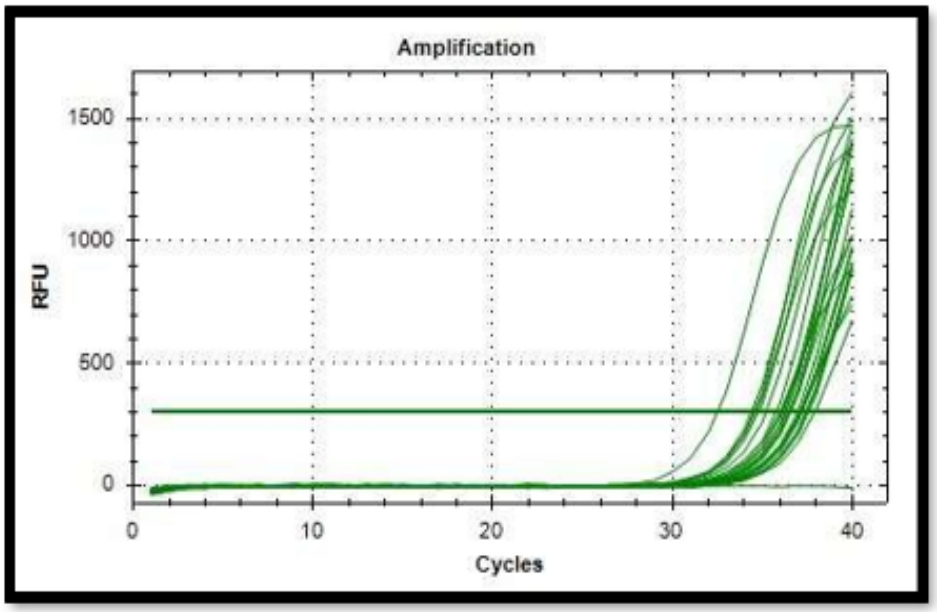


Figure (1) shows the RT-qPCR amplification curve for the study samples, with amplification beginning approximately between cycles 30 and 35.

The properties of double-stranded DNA (deoxyribonucleic acid) can be evaluated using melting curve analysis. This curve assesses the dissociation characteristics of DNA during heating; as the temperature rises, the double strands begin to separate, leading to an increase in absorbance (hyperchromicity). The temperature at which 50% of the DNA is denatured is known as the melting temperature, as illustrated in Figure (2).

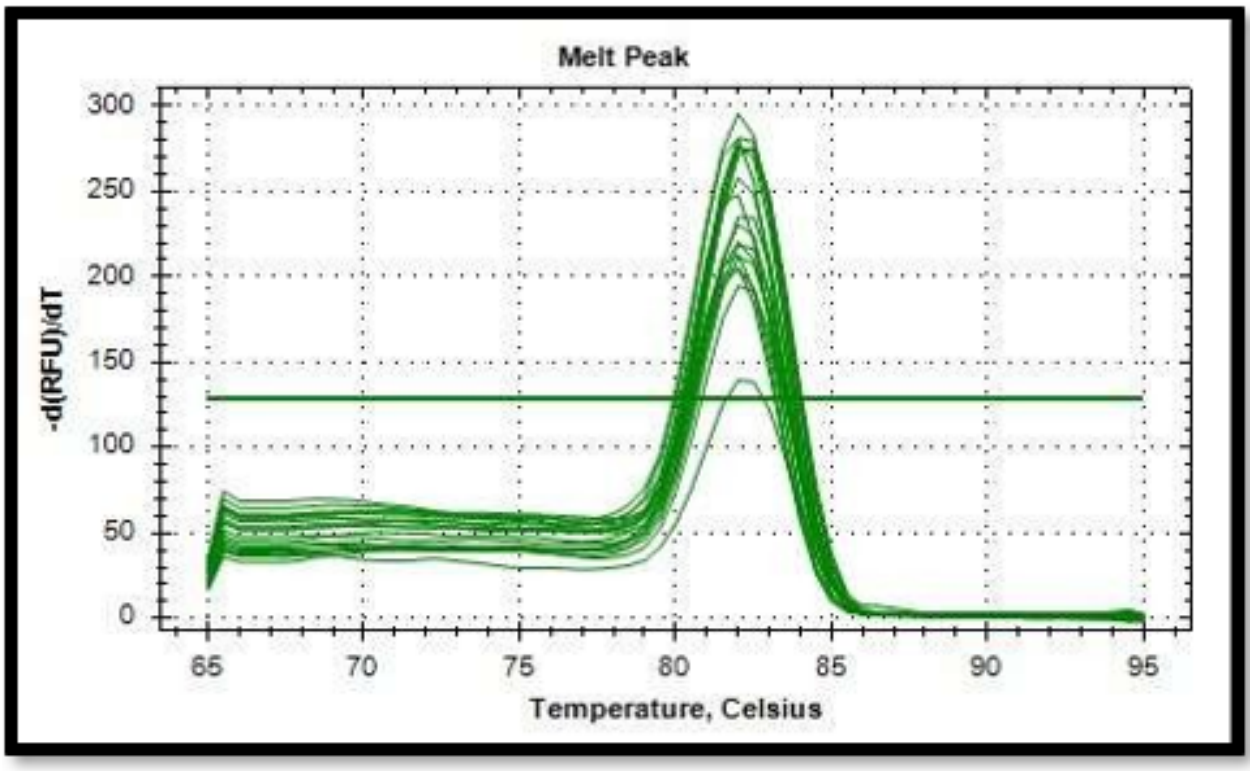


Figure (2) Melting peak curves of qPCR products for the study samples.

RT-qPCR analysis was performed on samples from the experimental groups across developmental stages using specific primers. At the embryonic stage (E14), the mean gene expression values (mean fold ± SD) were (0.94 ± 0.46) for the Saline group, (1.25 ± 1.03) for the SFN group, and (0.46 ± 0.32) for the RIS group. One-Way ANOVA results regarding *St8sia2* gene expression levels across the three experimental groups at stage E14 revealed no statistically significant differences between the Saline and SFN groups ($P = 0.5092$) or between the Saline and RIS groups ($P = 0.2103$). However, the comparison between the RIS and SFN groups yielded a statistically significant difference ($P = 0.0488$), as illustrated in Figure (3).

At the day of birth (P0), the mean value of gene expression for the Saline group was (1.06 ± 1.06), whereas the mean for the SFN group rose to (1.21 ± 1.05), while it decreased to (0.16 ± 0.23) in the RIS group. Statistical analysis revealed no significant difference between the Saline and SFN groups ($P = 0.9066$). Conversely, there were significant differences between the Saline and RIS groups ($P = 0.0360$) and between the RIS and SFN groups ($P = 0.0173$), Figure (4).

At the one-week postnatal stage (P7), the mean gene expression value for the Saline group was (1.18 ± 0.69), whereas the mean for the SFN group rose to (1.57 ± 1.11) while it dropped to (0.06 ± 0.07) in the RIS group. Statistical analysis revealed no significant difference between the Saline and SFN groups ($P = 0.3547$). Conversely, there were clear significant differences between the Saline and RIS groups ($P = 0.0012$), as well as between the RIS and SFN groups ($P = 0.0001$), as illustrated in Figure (5). It could be inferred that the observed downregulation of *St8sia2* expression at P0 and P7 might be associated with RIS exposure, or possibly influenced by underlying non-drug developmental variation.

Natural Resources for Human Health
eISSN: 2583-1194

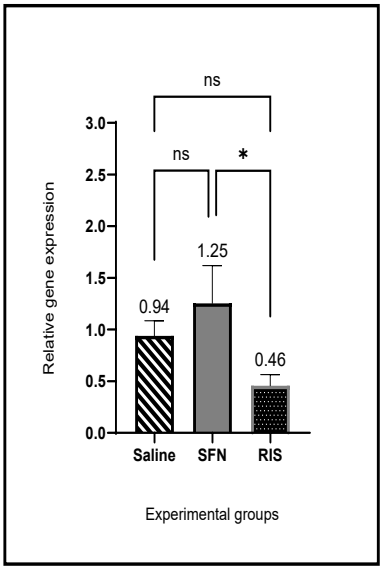


Figure (3) Gene expression levels of the *St8sia2* gene in experimental groups at stage E14.

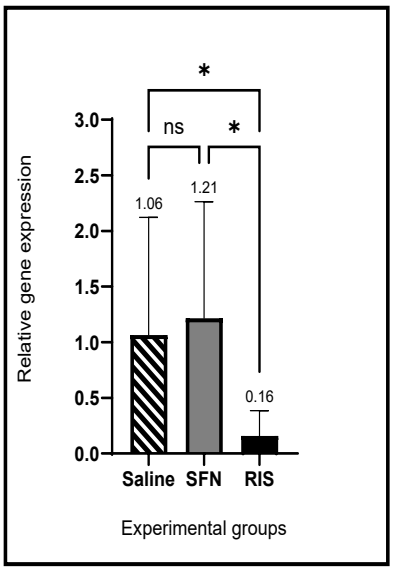


Figure (4) Gene expression levels of the *St8sia2* gene for the experimental groups at stage P0.

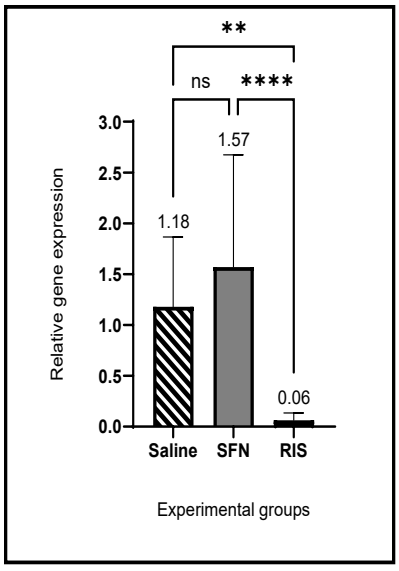


Figure (5) Gene expression levels of the *St8sia2* gene for the experimental groups at stage P7.

The results revealed a gradual upward trend in gene expression levels as developmental stages progressed, particularly in the control and sulforaphane groups; conversely, the risperidone group exhibited a numerical downward trend in gene expression from the embryonic stage (E14) through the stage immediately following birth (P0) to the one-week postnatal stage (P7). Comparisons showed no significant differences among the three stages, with all p-values exceeding 0.05 as shown in Table (3) and Figure (6).

Table (3) Results of multiple comparisons for *St8sia2* gene expression across developmental stages.

Treatment	Comparisons	Adjusted P Value
Saline	E14 vs P0	ns 0.9206
	E14 vs P7	ns 0.6863
	P0 vs P7	ns 0.8657
SFN	E14 vs P0	ns 0.9934
	E14 vs P7	ns 0.5202
	P0 vs P7	ns 0.3942
RIS	E14 vs P0	ns 0.6505
	E14 vs P7	ns 0.4504
	P0 vs P7	ns 0.9489

Natural Resources for Human Health
eISSN: 2583-1194

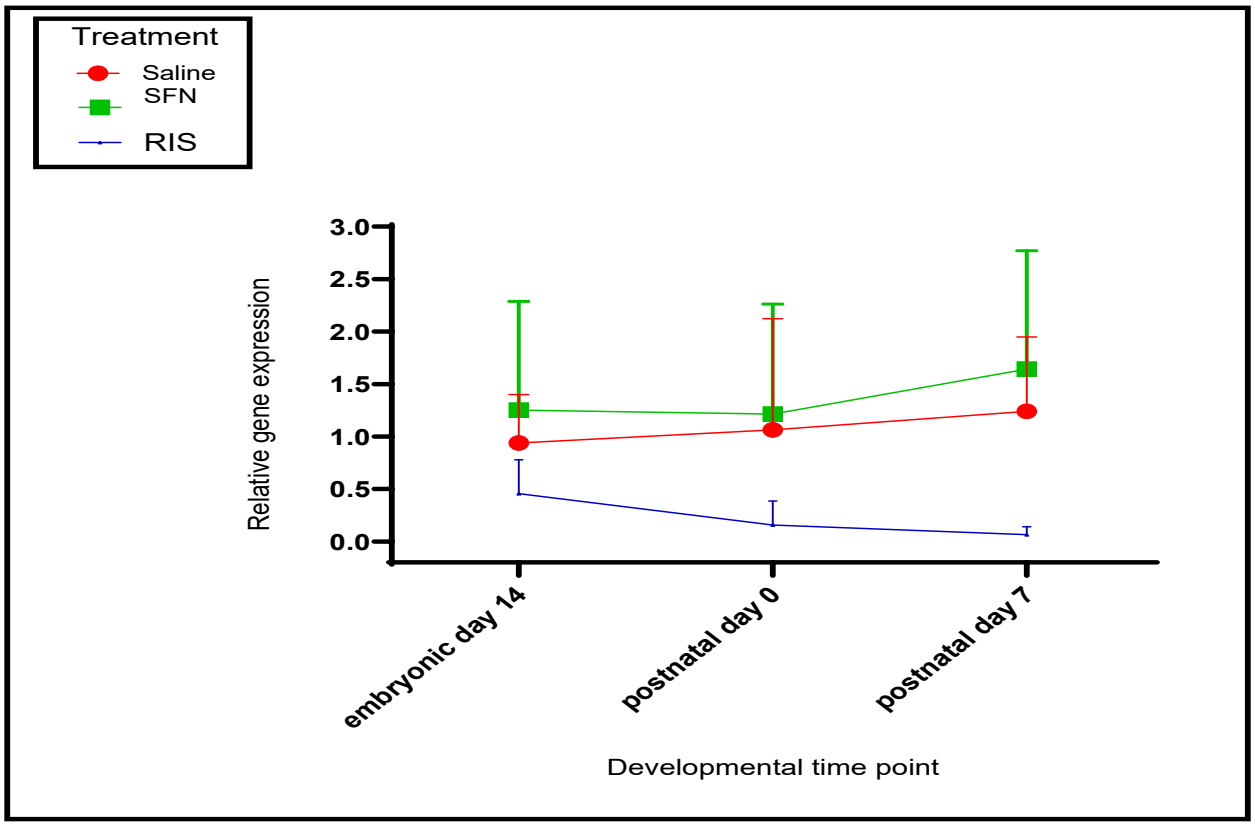


Figure (6) Changes in relative gene expression levels of the *St8sia2* gene during developmental stages

RT-qPCR analysis was performed on samples from the three groups across three time points using primers specific to the *St8sia4* gene. At the embryonic stage (E14), the mean gene expression values (mean fold ± SD) were (0.87 ±1.28) for the Saline group, (1.15 ± 0.81) for the SFN group, and (0.59 ± 0.31) for the RIS group. The results comparing *St8sia4* expression levels among the three experimental groups at stage E14 revealed no statistically significant differences (P = 0.7798) between the Saline and SFN groups, (P = 0.7498) between the Saline and RIS groups, and (P = 0.4476) between the RIS and SFN groups, as illustrated in Figure (7).

At the day of birth (P0), the mean value of gene expression for the Saline group was (0.81 ± 0.75); (1.05 ± 0.74) in the SFN group, (0.53 ± 0.28) in the RIS group. Statistical analysis revealed no significant differences between the Saline and SFN groups (P = 0.5904), no significant differences between the Saline and RIS groups (P = 0.4968), and no significant differences between the RIS and SFN groups (P = 0.1259), as illustrated in Figure (8).

At the one-week postnatal stage (P7), the mean gene expression value for the Saline group was (1.04 ± 0.75); the mean increased to (1.34 ± 0.98) in the SFN group, (0.24 ± 0.18) in the RIS group. Statistical analysis revealed no significant difference between the Saline and SFN groups (P = 0.4682). Conversely, significant differences were observed between the Saline and RIS groups (P = 0.0139) and between the RIS and SFN groups (P = 0.0004), Figure (9). The significant reduction in *St8sia4* expression observed exclusively at P7 suggests a potential time dependent sensitivity, which may possibly be linked to delayed transcriptional interference by RIS.

Natural Resources for Human Health
eISSN: 2583-1194

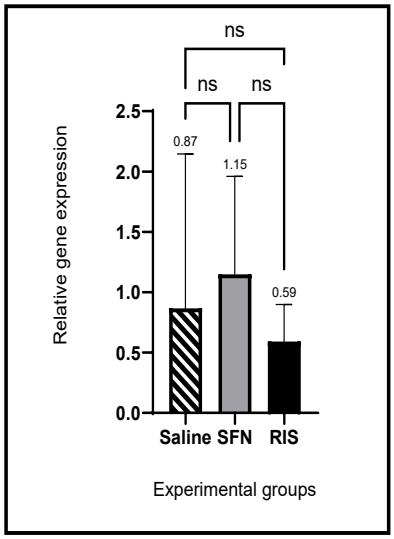


Figure (7) Gene expression levels of the *St8sia4* gene for the experimental groups at stage E14 .

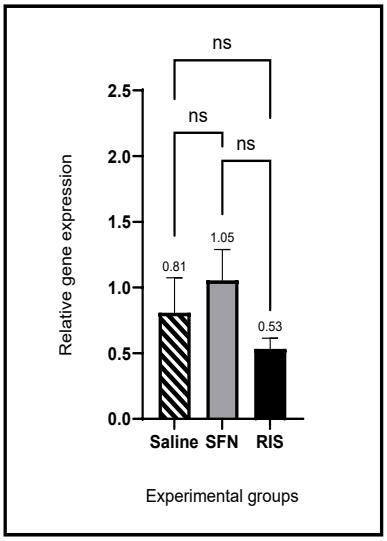


Figure (8) Gene expression levels of the *St8sia4* gene in experimental groups at stage P0.

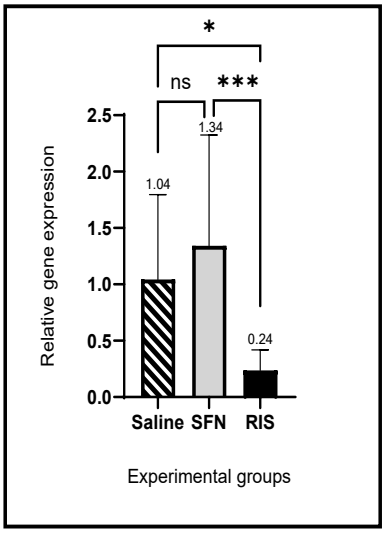


Figure (9) Gene expression levels of the *St8sia4* gene in experimental groups at stage P7.

Two-way ANOVA results indicated stable gene expression levels across developmental stages, particularly in the control and sulforaphane groups; conversely, the risperidone group exhibited a numerical downward trend in gene expression levels from the day-of-birth stage (P0) through the one-week post-natal stage (P7). Comparisons between developmental stages within each group using Tukey's multiple comparisons test revealed no significant differences among the three stages, with all p-values exceeding 0.05, as shown in Table (4). These results demonstrate that temporal changes in *St8sia4* gene expression levels within the study groups did not show significant variation as illustrated in Figure (10).

Table (4) Results of multiple comparisons for *St8sia4* gene expression across developmental stages.

Treatment	Comparisons	Adjusted P Value
Saline	E14 vs P0	ns 0.9865
	E14 vs P7	ns 0.8673
	P0 vs P7	ns 0.7615
SFN	E14 vs P0	ns 0.9649
	E14 vs P7	ns 0.8423
	P0 vs P7	ns 0.5896
RIS	E14 vs P0	ns 0.9811
	E14 vs P7	ns 0.4726
	P0 vs P7	ns 0.5383

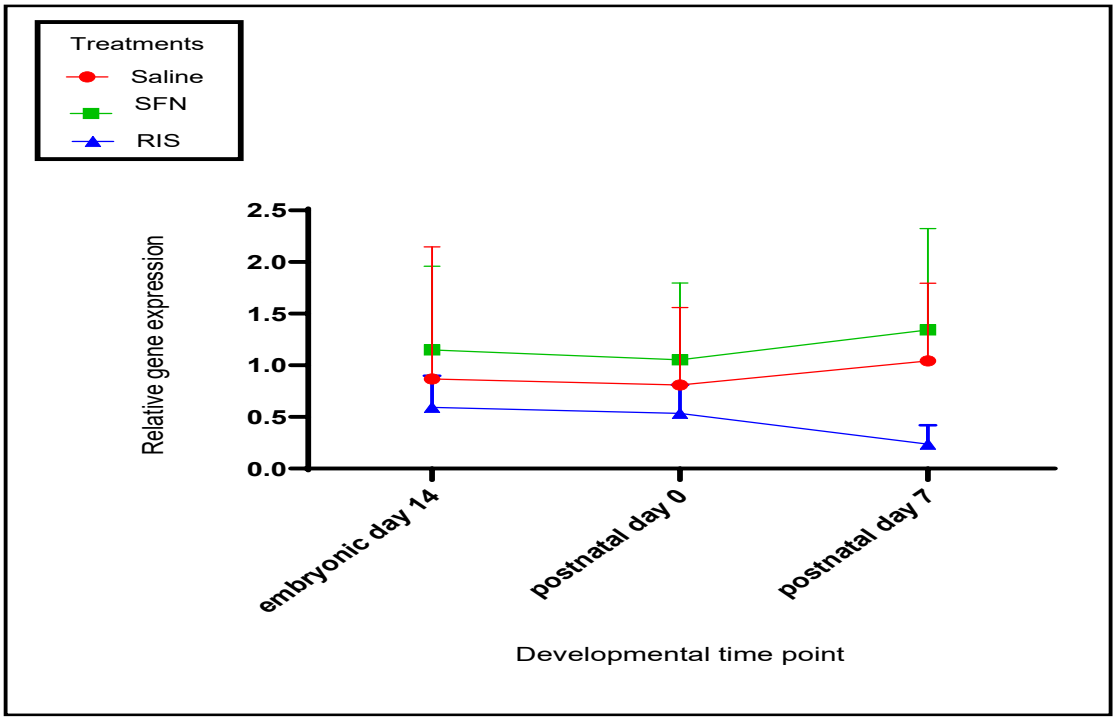


Figure (10) Changes in relative gene expression levels of the *St8sia4* gene during developmental stages.

Microscopic examination of brain tissue sections from rat fetuses and newborns (18 samples in total, across different developmental stages: E14, P0, P7) and three experimental groups: (Saline, SFN, RIS) revealed a positive reaction to the Periodic Acid-Schiff (PAS) stain, with varying intensity among groups. Purple staining of the intercellular matrix, neuronal membranes, and vascular cells is indicative of PAS-positive glycoconjugates (glycoproteins and related carbohydrates) during development. Histological examination of brain tissue from the control group (Saline) at E14 showed most neuroblasts and glioblasts were moderately stained with PAS, while nuclei exhibited blue counterstaining. Additionally, newly developed blood vessels and capillaries stained pink to purple, and brain tissue sections post-day 14 of gestation exhibited a uniform and intact cellular structure. The tissue was characterized by a high density of neurons and developing precursor cells (neuroblast-like and glioblast-like cells) with distinct round and oval nuclei arranged in an organized pattern, indicating cellular migration pathways and the onset of fiber bundle formation. The tissue also shows a positive PAS reaction in blood vessels and developing capillaries due to the glycoprotein-rich nature of their basement membranes, alongside positivity in the surrounding interstitial matrix, as shown in Figure (11).

In the Sulforaphane (SFN) group, histological section of the embryonic brain showed a marked positive PAS reaction, reflecting the distribution of glycoconjugates in the developing neural tissue. The tissue was densely cellular, containing closely packed cells. Some cells displayed darkly stained and condensed chromatin nuclei, suggesting possible mitotic activity of neural progenitor cells at this stage, which may reflect increased cellular proliferation. The heightened PAS intensity in the SFN group might indicate an enhanced accumulation of matrix glycoproteins rather than an alteration in cell membrane glycocalyx. Well-developed, packed neuroblasts stained positive with (PAS-positive) with a purple coloration corresponding to the glycosides covering the cell body (soma), along with intense staining of capillaries, as shown in Figure (12).

The histological section of the fetal brain in the Risperidone (RIS) group is characterized by a specific and normal positive PAS response, with moderate staining due to the presence of glycoproteins and embryonic interstitial matrix, which are a reflection of the biochemical distribution of the components of the developing nervous tissue, while the columns of migrating neurons and the neuroblast-like cells are characterized by the presence of a moderate pink cytoplasmic staining, with mild to moderate positivity in the surrounding interstitial matrix, alongside widened clear intercellular spaces, moderately PAS-stained neuroblasts and glioblasts, and strong pink staining of blood vessels, as shown in Figure (13).

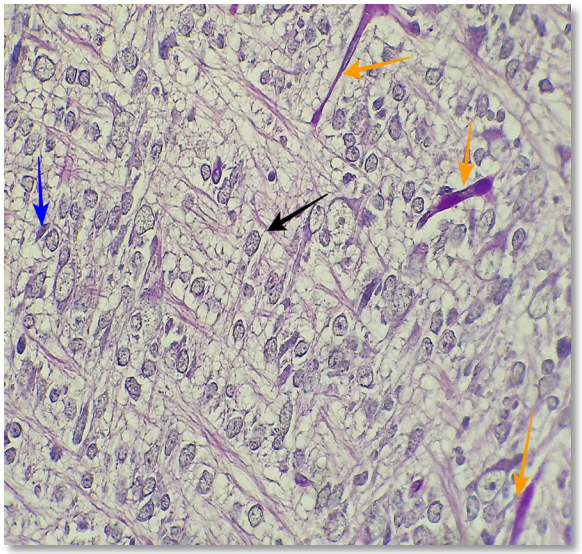


Figure (11): Brain tissue section of a 14-day-old rat fetus from the Saline group, showing the differential reactivity of developing nervous tissue components. Orange arrows indicate developing blood vessels and capillaries exhibiting intense positive staining; the blue arrow points to neuroblast-like cells; and the black arrow indicates densely packed developing glioblast-like cells, which show moderate positive reactivity to PAS staining (400x) .

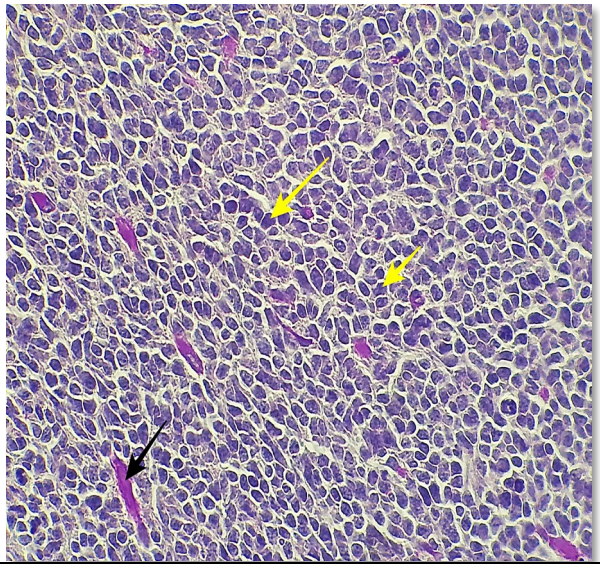


Figure (12): Brain tissue section of a 14-day-old rat fetus from the SFN group, showing the differential reactivity of developing neural tissue components. Yellow arrows indicate densely packed, PAS-positive neuroblast-like cells with darkly stained condensed nuclei, while the black arrow points to developing capillaries that are intensely stained with PAS due to glycoprotein deposition in the basement membrane (400x) .

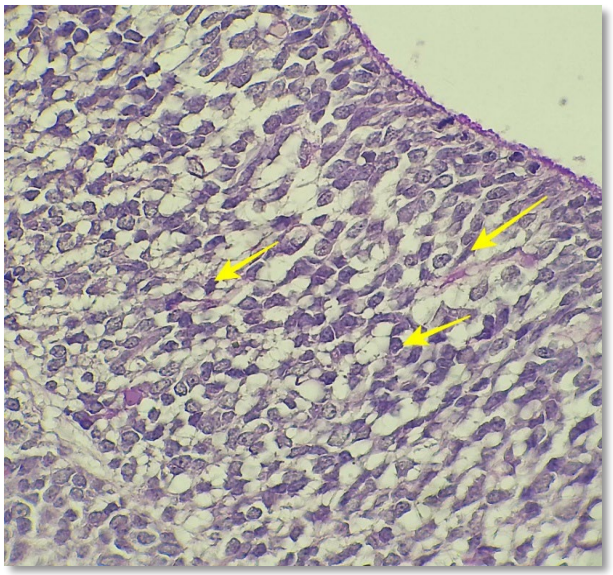


Figure (13): Brain tissue section of a 14-day-old rat fetus from the RIS group, showing the differential reactivity of the developing nervous tissue components to PAS staining. Yellow arrows indicate negative to weak staining of neurons and glial cells, while their nuclei stained blue, blood vessels exhibited strong staining as a violet color, and neuroblast-like cells with densely stained nuclei distributed among widened intracellular spaces (400x).

For the results obtained at birth (P0/day of birth), light microscopy examination of brain section from the control group (saline-treated) demonstrated distinctive histological characteristics under PAS staining. A clear contrast in staining intensity was

observed, transitioning to moderate and faint levels within the tissue matrix and glial cells. Reflecting a moderate distribution of cytoplasmic carbohydrates and growth-associated glycoproteins throughout the developing nervous tissue. The basement membrane of developing blood vessels in the brain appeared bright pink, well-defined, and intensely stained, indicating that the vascular network is in an active growth phase (angiogenesis). Meanwhile, neuronal nuclei were stained dark blue as shown in Figure (14).

In the Sulforaphane (SFN) group at birth (P0), microscopic examination of the PAS-stained tissue section revealed marked variations in color reaction intensity. Concentrated strong purple staining was observed in the basement membranes and walls of blood vessel and developing capillaries, owing to their high glycoprotein content associated with vascular development. Moderate staining of glycoprotein deposits was noted in glial cell. Furthermore, a strong reaction was detected in neuronal nuclei which stained deep blue, while some neurons exhibited cytoplasmic vacuolization, as shown in Figure (15).

Regarding the Risperidone (RIS) group at birth (P0/ day of birth), microscopic examination of the nervous tissue reveals distinct patterns of cellular reactivity under PAS staining. Areas of high cellular density packed immature neurons and glioblast with dark chromatin-dense nuclei. Neurons and most glial cells showed negative to weak cytoplasmic staining, whereas some glial cells exhibited positive PAS reactivity, while their nuclei stained blue. Conversely, the developing blood vessels and capillaries exhibited strong PAS positive, with endothelial walls and basement membranes staining a distinct purple to violet color, reflecting a high content of carbohydrates and glycoproteins associated with active angiogenesis during this early developmental stage. Developing astrocytes were also observed with pale, spherical, vesicular nuclei and a faintly reactive, spider-web or spongy cytoplasmic network within the neuropil. Interspersed among these were cells with elongated or spindle-shaped cytoplasmic processes (pyramidal-shaped cells) exhibiting weak to moderate staining reactivity, indicating early structural differentiation and development of neural tissue components, as shown in Figure (16).

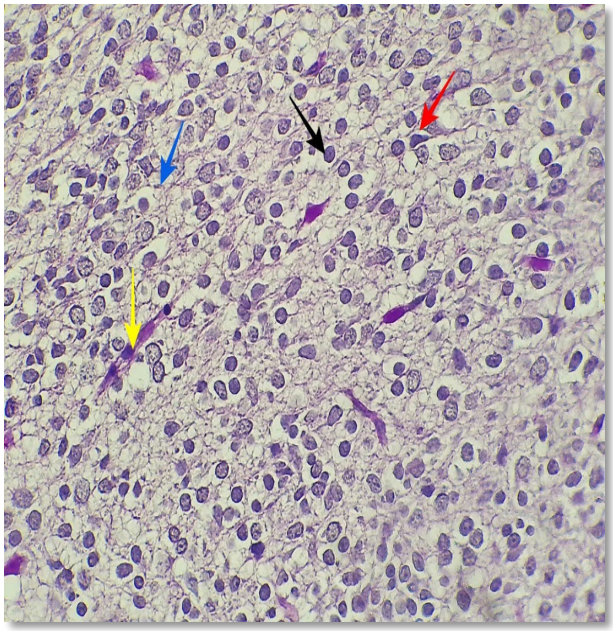


Figure (14): Brain tissue section of a neonatal rat from the Saline group, at day of birth (P0), showing the differential reactivity of the developing nervous tissue components. Black arrows indicate the closely packed, dark nuclei of neurons and glial cells, which are negatively reactive to the PAS stain; yellow arrows point to basement membranes of developing blood vessels, which exhibit a strong positive reaction to the stain; blue arrows indicate neuronal processes; and red arrows point to a pyramidal-shaped neuron (400x) .

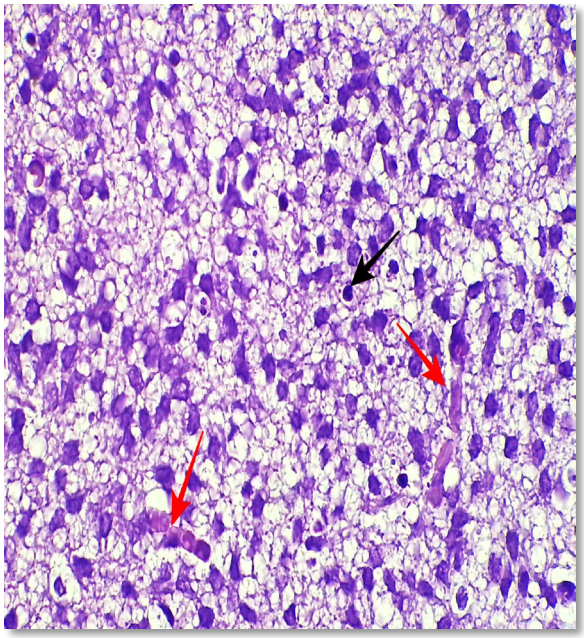


Figure (15): Brain tissue section of a neonatal rat from the SFN group, at day of birth (P0), showing the differential reactivity of developing neural tissue components. The black arrow indicates PAS-positive glial cell, while the red arrows point to the basement membranes of developing blood vessels, which exhibit a strong positive reaction to the stain (400x)

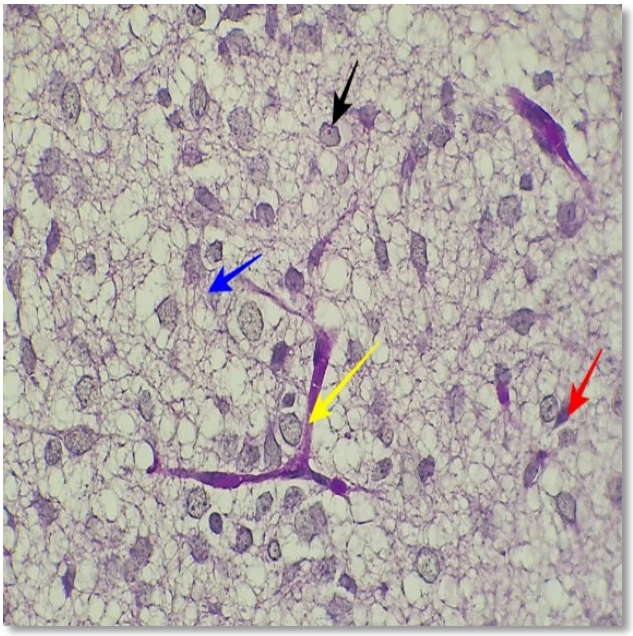


Figure (16): Brain tissue section of a young rat from the RIS group, at day of birth (P0), showing the differential reactivity of developing nervous tissue components. The black arrow indicates glial cells that are PAS-positive, while the yellow arrow points to the basement membrane of developing blood vessels, which exhibits a strong positive reaction to the stain. The blue arrow indicates neuronal processes, and the red arrow points to negative to weak staining of neurons and glial cells, as well as a pyramidal-shaped neuron (400x).

Microscopic examination of PAS stained brain section from rat pups at postnatal day 7 (P7) revealed clear differences in tissue reactivity among the groups. In the control group, regions of high cellular density were observed, consisting of closely packed pyramidal neurons with strongly PAS-positive (purple) cytoplasm and dark, chromatin-dense nuclei. The neurons were surrounded by PAS-positive material. Developing blood vessels and capillaries showed strong PAS positivity, with normal outlines and distinctly stained endothelial walls and basement membranes, reflecting a high content of carbohydrates and glycoproteins. Glial cells were identified by pale, rounded, vesicular nuclei within a faintly reactive, spongy neuropil, and were interspersed with cells bearing extended cytoplasmic processes that showed moderate reactivity (PAS stain, 400x), in Figure (17).

In the sulforaphane (SFN) group, sections showed a distinct positive PAS reaction, with strongly stained pyramidal neurons and an intensely reactive neuropil, consistent with a high glycoprotein content. Capillaries within the tissue were also PAS-positive, as their endothelial lining and basement membranes are rich in glycoproteins, and glial cells were clearly demonstrated and PAS-positive, see Figure (18).

In the risperidone (RIS) group, PAS-stained sections showed a strong reaction in developing capillaries and basement membranes, owing to the glycoprotein-rich nature of their basement membranes. Pyramidal neurons, axon hillocks, and their processes exhibited a moderate reaction, whereas staining in the neuropil and glial cells ranged from moderate to faint, indicating a lower cytoplasmic carbohydrate content in the nervous tissue compared with the other groups, see Figure (19).

The histochemical evaluation and diagnosis were primarily based on the detection and intensity of glycoproteins, which constitute an essential structural component of the cell glycocalyx and basement membranes, thereby reflecting the physiological and biochemical status of the developing neural tissue. Overall, the SFN group showed the most intense PAS reactivity, the control group showed a strong to moderate reaction, and the RIS group showed the weakest reaction. These differences may reflect altered glycoprotein content related to the expression of *St8sia2* and *St8sia4*, which encode sialyltransferases involved in the polysialylation of Neural Cell Adhesion Molecules (NCAM); however, PAS reactivity indicates total carbohydrate and glycoprotein content and does not specifically detect polysialic acid.

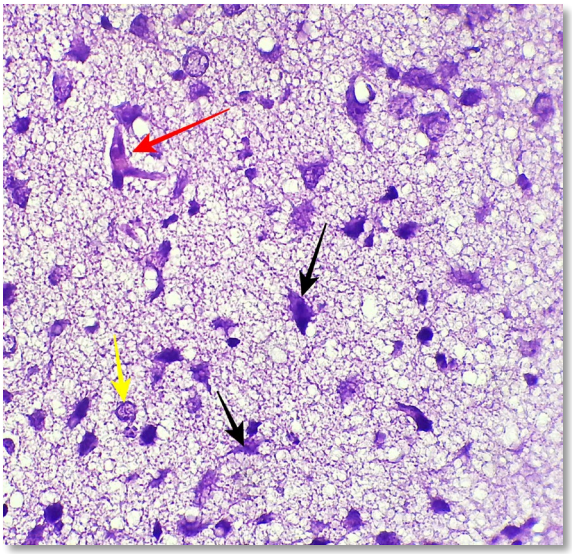


Figure (17): A section of brain tissue from a rat pup in the control group (saline) one week after birth, showing the differential reactivity of neural tissue components. The black arrows point to PAS-positive pyramidal neurons, and the yellow arrow points to glial cells, and the red arrow indicates the basement membranes of blood vessels, which exhibit a strong positive reaction to the stain (400x).

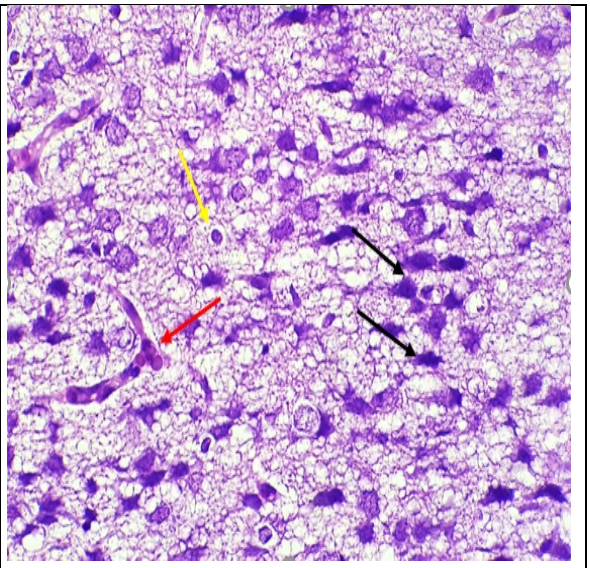


Figure (18): A section of brain tissue from the SFN group, one week after birth, showing the differential staining reaction of neural tissue components. The black arrows point to PAS-positive pyramidal neurons, the red arrow point to developing capillaries, and the yellow arrow indicates clearly demonstrated, PAS-positive glial cells (400x).

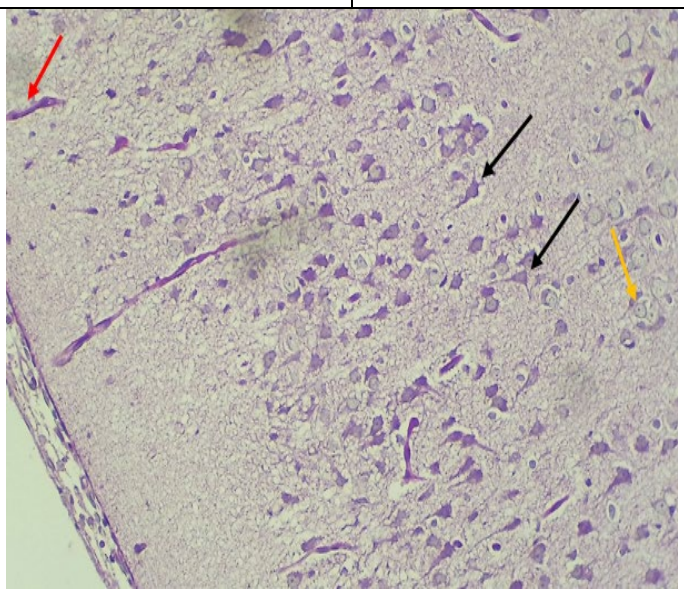


Figure (19): A section of brain tissue from a rat pup in the RIS group, one week after birth, showing the differential staining reaction of neural tissue components. The black arrows point to pyramidal neurons and their processes, which show a moderate reaction to the PAS stain; the yellow arrow indicates glial cells with a moderate to faint reaction; and the red arrow points to the basement membranes of blood vessels, which exhibit a strong positive reaction to the stain (400x).

DISCUSSION

The present study showed a developmental-stage-dependent pattern of the *St8sia2* and *St8sia4* gene expression after maternal exposure to sulforaphane (SFN) and risperidone (RIS). At E14, RIS and SFN only differed significantly. An early effect of RIS is therefore only suggested. (Schuster et al., 2020) demonstrated loss of *St8sia2* in mice changed the directional persistence and branching behavior of migrating interneurons and affected the distribution of parvalbumin-positive interneurons in the developing cortex. At P0, *St8sia2* expression in the RIS group declined further compared with the embryonic stage, whereas the Saline and SFN groups showed slightly higher mean expression. This finding suggests that the lower *St8sia2* expression associated with RIS exposure was more pronounced around the time of birth, although the within-group changes across developmental stages were not statistically significant. This timing is notable because *St8sia2* is especially important during embryonic and perinatal development. (Curto et al., 2019) reported that *St8sia2* expression is prominent in embryonic and perinatal stages and declines afterward, whereas *St8sia4* has a relatively different temporal profile. (Mori et al., 2017) showed that although both enzymes are involved in polySia synthesis, *St8sia2* and *St8sia4* produce polysialic acid chains with different characteristics. Moreover, (Szewczyk et al., 2017) showed that *St8sia2* deficiency in mice was associated with impaired oligodendrocyte differentiation, reduced myelin content, thinner myelin sheaths, and axonal abnormalities. (Werneburg et al., 2017) demonstrated that the two polysialyltransferases have opposing effects during oligodendrocyte differentiation, with *St8sia2* supporting early oligodendrocyte differentiation, whereas *St8sia4* becomes more prominent during later stages. (Küçükerden et al., 2022) showed that selective deletion of *St8sia2* in different brain regions resulted in abnormalities in particular neural pathways, including the mammillary body and mammillothalamic tract, and was linked to altered behavioral phenotypes. (Curto et al., 2019) showed that *St8sia4* depletion led to reduced dendritic complexity, while depletion of either *St8sia2* or *St8sia4* affected the density of parvalbumin-positive perisomatic synaptic structures. These results suggest that the two enzymes can contribute both overlapping and distinct contributions to neuronal connectivity. The current findings are also consistent with previous empirical evidence on prenatal RIS exposure. (Singh et al., 2016) reported developmental neurotoxicity induced by prenatal RIS exposure in rats including decrease in fetal brain size and weight, changes in neocortical architecture and apoptotic neurodegeneration. In a related study, (Singh and Singh, 2017) reported that in utero RIS exposure produced structural abnormalities in the developing hippocampus and striatum and was associated with cognitive impairment in offspring. (Han et al., 2017) reported that low concentrations of SFN promoted neural stem-cell proliferation and neuronal differentiation and were associated with activation of Wnt signaling. In addition, dietary bioactive compounds, including isothiocyanates such as sulforaphane, have been proposed to modulate gene expression through epigenetic mechanisms such as the regulation of DNA methyltransferase activity (Campisi et al., 2025). Therefore, the relatively higher expression values observed in the SFN group may be compatible with a broader neurobiological effect of SFN, but the present data do not establish a direct effect of SFN on *St8sia2* or *St8sia4* transcription.

Histological results using PAS staining showed that the control group maintained normal glycoprotein distribution and tissue architecture. At P7, PAS reactivity was most intense in the SFN group, moderate to strong in the control group, and weakest in the RIS group, whereas the basement membranes of developing capillaries showed a strong reaction in all groups. Numerous previous studies support the neuroprotective properties of sulforaphane, a natural isothiocyanate. For example, (Fahey et al., 2025) reported that sulforaphane protects the nervous system against the toxic effects of environmental pollutants and counteracts tissue and cellular damage caused by advanced glycation end-products by facilitating detoxification. Another study reported that sulforaphane protects nervous tissue, and consequently neurons, from oxidative stress-induced apoptosis by upregulating intracellular antioxidant enzymes and reducing reactive oxygen species, and histological analysis following treatment revealed improved neuronal survival and reduced degeneration (Tarozzi et al., 2013). In contrast, the reduced *St8sia2* and *St8sia4* expression associated with maternal risperidone exposure may translate into lower sialic acid and polysialic acid synthesis in developing fetal and neonatal brains, which could disrupt neuronal glycoprotein integrity and impair cellular migration and tissue architecture. However, this remains a hypothesis, as sialyltransferase activity and polysialic acid levels were not measured in this study. Previous studies have shown that in utero risperidone exposure induces structural abnormalities in the fetal and offspring hippocampus, striatum, and neocortex (Singh et al., 2016; Singh and Singh, 2017). The PAS pattern observed here is directionally consistent with the gene expression finding, in which RIS was associated with reduced *St8sia2* expression around birth, whereas the SFN group showed slightly higher mean expression. However, PAS reactivity reflects total carbohydrate and glycoprotein content and cannot be attributed specifically to polysialylation, so the link between the altered *St8sia2* and *St8sia4* expression and the observed staining remains suggestive rather than causal. In this study, Periodic Acid-Schiff (PAS) staining was employed under light microscopy to evaluate tissue glycoproteins and carbohydrate-conjugated

molecules within the developing brain tissue. While PAS staining effectively demonstrates the accumulation and distribution of glycoprotein-rich matrix components, it provides a broader histological view rather than the specific ultrastructural dimensions of the cellular glycocalyx layer. It is worth noting that a definitive, ultra-high resolution quantitative measurement of the membrane glycocalyx layer strictly requires Transmission Electron Microscopy (TEM). Due to the limited access to TEM facilities during the study, our evaluation was limited to light microscopic evaluation using PAS staining, focusing primarily on glycoprotein constituents.

Ethical Approval: This study was approved by the Animal Ethics Committee, College of Veterinary Medicine, Tikrit University, Iraq (Approval No.: Tu.Vet.161, dated December 17, 2025).

REFERENCES

[1] Al-Hajj, H. A. (2010). Light Microscopic Preparations: Theory and Practice. Dar Al-Masirah for Publishing, Distribution, and Printing. First Edition, Amman, Jordan, 238.

[2] Bessetti, R. N. & Litwa, K. A. (2025). Broccoli for the brain: a review of the neuroprotective mechanisms of sulforaphane. *Frontiers in Cellular Neuroscience*, 19, 1601366.

[3] Campisi, M., Cannella, L., Visioli, F. & Pavanello, S. (2025). Mechanistic insights and perspectives for healthy aging. *Advances in Nutrition*, 100521.

[4] Curto, Y., Alcaide, J., Röckle, I., Hildebrandt, H. & Nacher, J. (2019). Effects of the genetic depletion of polysialyltransferases on the structure and connectivity of interneurons in the adult prefrontal cortex. *Frontiers in Neuroanatomy*, 13, 6.

[5] Fahey, J. W., Liu, H., Batt, H., Panjwani, A. A. & Tsuji, P. (2025). Sulforaphane and brain health: from pathways of action to effects on specific disorder. *Nutrients*, 17(8), 1353.

[6] Foote, C. A., Soares, R. N., Ramires-Peres, F. I., Ghiarone, T., Aroor, A., Manrique-Acevedo, C., Padilla, J. & Martinez-Lemus, L. A. (2022). Endothelial Glycocalyx. *Comprehensive Physiology*, 12(14), 3781-3811.

[7] Han, Z., Xu, Q., Li, C. & Zhao, H. (2017). Effects of sulforaphane on neural stem cell proliferation and differentiation. *Genesis*, 55, e23022.

[8] Küçükerden, M., Schuster, U., Röckle, I., Alvarez-Bolado, G., Schwabe, K. & Hildebrant, H. (2022). Compromised mammillary body connectivity and psychotic symptoms in mice with di- and mesencephalic ablation of ST8SIA2. *Translational Psychiatry*, 12(1), 51.

[9] Livak, K. J. & Schmittgen, T. D. (2001). Analysis of relative gene expression data using real-time quantitative PCR and the $2^{(-\Delta\Delta Ct)}$ method. *Methods*, 25(4), 402-408.

[10] Macklin Biochemical. (2025a). DL-Sulforaphane 97% (CAS No. 4478-93-7; Cat. No. D818039): Technical Specification and Product Data Sheet. Shanghai Macklin Biochemical Co., Ltd., Shanghai, China.

[11] Macklin Biochemical. (2025b). Risperidone 99% (CAS No. 106266-06-2; Cat. No. R832185): Technical Specification and Product Data Sheet. Shanghai Macklin Biochemical Co., Ltd., Shanghai, China.

[12] Möckl, L. (2020). The Emerging Role of the Mammalian Glycocalyx in Functional Membrane Organization and Immune System Regulation. *Frontiers in Cell Developmental Biology*, 8, 253.

[13] Mori, A., Hane, M., Niimi, Y., Kitajima, K. & Sato, C. (2017). Different properties of polysialic acids synthesized by the polysialyltransferases ST8SIA2 and ST8SIA4. *Glycobiology*, 27(9), 834-846.

[14] Okab, A. M., El-Kattan, A. K., Salem, M. F. & Azzam, A. R. (2025). The potential teratogenicity of atypical antipsychotic drugs olanzapine versus risperidone on the fetuses and placentae of the pregnant female albino rats: Anatomical and histological study. *Tanta Medical Journal*, 53(3), 386-394.

[15] Richter, J. R. & Sanderson, R. D. (2023). The Glycocalyx: pathobiology and repair. *Matrix Biology Plus*, 17, 100128.

[16] Schnaar, R. L., Gerardy-Schahn, R. & Hildebrandt, H. (2014). Sialic acids in the brain: gangliosides and polysialic acid in nervous system development, stability, disease, and regeneration. *Physiological Reviews*, 94(2), 461-518.

[17] Schuster, U. E., Rossdam, C., Röckle, I., Schiff, M. & Hildebrandt, H. (2020). Cell-autonomous impact of polysialic acid producing enzyme ST8SIA2 on developmental migration and distribution of cortical interneurons. *Journal of Neurochemistry,* 152, 333–349.

[18] Singh, K. P. & Singh, M. K. (2017). In utero exposure to atypical antipsychotic drug, risperidone: effects on fetal neurotoxicity in hippocampal region and cognitive impairment in rat offspring. *Progress in Neuro-Psychopharmacology & Biological Psychiatry*. 77, 238-249.

[19] Singh, K. P., Singh, M. K. & Singh, M. (2016). Effects of prenatal exposure to antipsychotic risperidone on developmental neurotoxicity, apoptotic neurodegeneration and neurobehavioral sequelae in rat offspring. *International Journal of Developmental Neuroscience*, 52, 13–23.

[20] Szewczyk, L. M., Brozko, N., Nagalski, A., Rockle, I., Werneburg, S., Hildebrandt, H., Wisniewska, M. & Kuznicki, J. (2017). ST8SIA2 promotes oligodendrocyte differentiation and the integrity of myelin and axons. *Glia*, 65(1), 34–49.

[21] Tarozzi, A., Angeloni, C., Malaguti, M., Morroni, F., Hrelia, S. & Hrelia, P. (2013). Sulforaphane as a potential protective phytochemical against neurodegeneration diseases. *Oxidative Medicine and Cellular Longevity*, 2013(1), 415078.

[22] Werneburg, S., Fuchs, H., Albers, I., Burkhardt, H., Gudi,V., Skripuletz, T., Stangel, M., Gerardy-Schahn, R. & Hildebrandt, H. (2017). Polysialylation at early stages of oligodendrocyte differentiation promotes myelin repair. *Journal of Neuroscience*, 37(34), 8131–8141.

[23] Yoo, S. W., Motari, M. G., Susuki, K., Prendergast, J., Mountney, A., Hurtado, A. & Schnaar, R. (2015) Sialylation regulates brain structure and function. *The FASEB Journal*. 29(7), 3040.

[24] Zhu, W., Zhou, Y., Guo, L. & Feng, S. (2024). Biological function of sialic acid and sialylation in human health and disease. *Cell Death Discovery*, 10(1), 415.